View metadata, citation and similar papers at core.ac.uk
brought to you by CORE
provided by Engineering Journal (Faculty of Engineering, Chulalongkorn University, Bangkok)

Engineering Journal issn: 0125-8281

Article

Parameter Tuning of the Autonomous Boat in Fish Farming Industry with Design of Experiment

Mongkol Thianwiboon

Department of Industrial Engineering, Faculty of Engineering, Mahidol University, Nakorn Pathom 73170, Thailand
E-mail: mongkol.thi@mahidol.ac.th

Abstract. This research studied the feasibility in applying the flight controller of the unmanned aerial vehicle on a pontoon boat in fish farming industry. A small-scale autonomous pontoon boat has been built, equipped with the open-hardware flight controller, GPS receiver, Inertial Measurement Units (IMU) and the magnetometer.

A 2^3 factorial design based on Design of Experiment (DOE) is carried out to study the influence of three parameters (turn_rate, turn_angle and damping) on the response variable (peak-to-peak deviation from the desired trajectory). Total 24 experiments have been conducted by setting the desired trajectory as a circle with diameter 20 m. The peak-to-peak deviation in each experiment has been observed.

The analyses revealed that the damping has low interaction with the turn angle and turn rate while there is a stronger interaction between the turn angle and turn rate. And the peak-to-peak deviation of the trajectory tends to decrease when the parameter damping was set to high value. The regression model has been derived and plotted as a response surface. The optimized parameters were selected from the plot and perform the experiment with three replications. The results confirm that parameters tuning has improved the performance of the boat significantly.

With the DOE approach, the impact of two or more parameters on a response, the interaction between parameters can be investigated systematically. This approach is an effective way to tuning the parameters and can be applied to various kinds of the autonomous vehicle.

Keywords: Underwater ploughing, autonomous surface vehicle, ASV, design of experiments, DOE.

ENGINEERING JOURNAL Volume 24 Issue 5
Received 31 January 2020
Accepted 3 August 2020
Published 30 September 2020
Online at https://engj.org/
DOI:10.4186/ej.2020.24.5.217

DOI:10.4186/ej.2020.24.5.217

1. Introduction

Aquaculture is probably the fastest growing food production sector. Total aquaculture supply accounts for half of the world's fish that is used for food. In 2012, the Asia–Pacific region accounts for 88.5 percent of global production [1]. Adoption of Genetically Improved Farm Tilapia (GIFT) was a key development that fueled rapid growth of tilapia farming. In 2012, more than half of the GIFT production in Asia comes from major producers such as China, the Philippines, Indonesia and Thailand [2]. In Thailand, most tilapia farms are earthen pond culture which their waste and disease is contained in the pond not spread to the environment [3]. Earthen pond culture also suffers less from diseases and parasites compare to floating cage in the river due to the controllable, high quality environment and reducing handling stress [4]. However, in the high-density pond, heavily fish stocking and high feed supply leads to the excess, unconsumed feeds decompose at the pond bottom by aerobic micro-organisms and pollute the water [5].

The most important parameter of water quality is the dissolved oxygen (DO) [6,7]. And the growth performance of tilapia also found to be significantly higher with DO in aerated ponds compared to the non-aerated ponds [8-11].

Paddlewheels are most widely used to infuse oxygen into the water and increase circulation of water [12]. However, circulation can result in erosion of the embankments, and deposition of sediments in the center of the pond where water velocities are lowest [13,14]. Furthermore, large air bubbles created by the rotating paddle wheel escape the water too quickly and do not aerate down to the bottom of the pond where oxygen is needed most. Thus, bottom aerators, such as diffused-air and propeller-aspirator pumps have been used to aerate down to the bottom of the pond, shifting bacteria from anaerobic to aerobic types, producing harmless and odorless carbon dioxide waste gases. [6, 15].

Underwater ploughing can also be used to disturb the surface of the pond soil, encourage movement of oxygenated water into the soil mass. Underwater ploughing can supply oxygen to the pond soil a minimum of erosion and water losses [16, 17].

Underwater ploughing is widely used in shrimp farming in Thailand by dragging rake and chains over pond bottom to scarify surface soil with a pontoon boat. This process is done in daily or weekly period especially at the center of the pond. The continuous movement of water help to release the nutrients, improving health and color as well as reduces the amount of muck and sludge [18-22].

P.Charoen Farm, one of the biggest tilapia farming in Thailand adopted the underwater ploughing with the pontoon boat similar to the shrimp farm to stir and make the soil sediment to float up and mix with oxygen conjunction with using pro-biotics to improve water quality. The boat operation in the pond and CAD model of the boat shown in Fig. 1.

(a) The boat dragging rake and chains

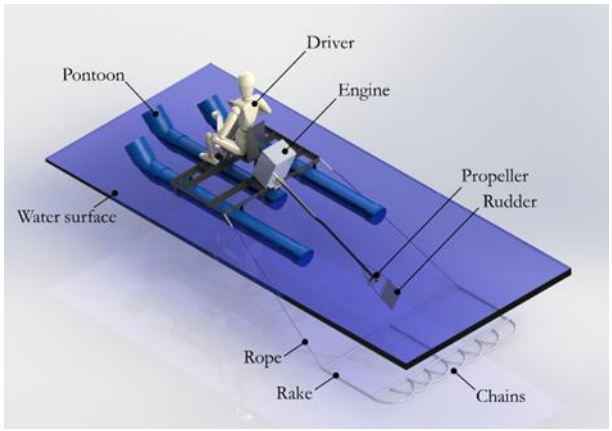

(b) The CAD model showing the boat, rake and chains

Fig. 1. Underwater ploughing using the pontoon boat in the tilapia pond.

The treatment using the underwater ploughing with a pontoon boat takes about 48 hours for a pond with 3000 square meters surface area. The boat's driver has to work in outdoor amidst sunlight and receive vibrations from the engine during this period. To shift the worker for more value-added work, the Autonomous Surface Vehicle (ASV) is suitable to implement in this process.

The first step of the study was building the small-scale pontoon boat similar to the one used in tilapia farming and use as an experimental system. After that, converted it into an ASV by establishing motion control with various sensors. Since the characteristics of the system is quite complex, the parameter tunings with mathematical model become difficult. One-factor-at-a-time approach also not suitable because it neglects the interaction between parameters that might change the behavior of the system. Thus, the parameter tunings in this study are based on the Design of Experiment (DOE) approach to systematically study the influence of the selected control parameters on the response variable. Analysis of variance (ANOVA) is also used to investigate and model the relationship between the response variable and one or more independent parameters.

Once the analyses were completed, the ASV was set with the new optimized parameters obtained from the

regression model. The additional experiments were performed to validate the accuracy of the model.

This approach is an effective way to tuning the parameters and can be applied to various kinds of the autonomous vehicle.

2. Motion Control Background

Proportional navigation which is previously used in missiles guidance algorithm is widely accepted as the preferred method of guidance [23-25]. Motivated by this navigation, Sanghyuk, John & Jonathan of MIT presented a new nonlinear guidance for trajectory tracking of the unmanned air vehicles (UAVs) [26].

An algorithm to determine boat headings with various sensors, such as GPS receiver and wind sensor for an autonomous sailboat is introduced in 2008 [27]. Cruz and Alves developed an auto-heading controller with a simple dynamic model relied only on data that were available with low-cost sensors in 2010 [28]. Simple control algorithms with few parameters for an autonomous sailboat also proposed by Clement [29].

Around 2005 to 2010, advances in electronics allowed the production of cheap GPS receiver, accelerometers/inertial measurement unit (IMU), magnetometer (compass) and high performance, lightweight flight controllers. This resulted in popularity of the autonomous vehicles.

The use of GPS receiver, Inertial Navigation System (INS) and ground control station software "Mission Planner" with Google Maps enable an Unmanned Ground Vehicle (UGV) to perform variety of tasks [30]. Ullah & Abdullah also developed an autonomous surveying boat which follows a predefined path while getting the coordinates and direction from GPS receiver and magnetometer (compass) respectively [31]. Furthermore, Giron-Sierra, Gheorghita, Angula & Jimenez proposed the use of two autonomous boats for towing a boom for oil spill recovery in 2015. Simulations and experiments with a scaled boat towing a boom were performed to support their research [32]. A scaled autonomous sailboat which capable to sail along the predefined path using only the sails as propulsion also developed by Stenersen in 2016 [33]. Two years later, Zhang & Hsu developed the Kalman filter and adaptive tuning and applied in the low-cost quadcopter with the commercial flight control Pixhawk® equipped with GPS receiver, IMU and magnetometer [34]. The fuzzy logic landing system for Quadcopter based on laser rangefinder is developed in 2019 and implemented with the Pixhawk® flight controller.

Nowadays, the Pixhawk® is widely used to control most of the unmanned vehicle. The nonlinear guidance logic proposed by Sanghyuk et al. [26] become the fundamental for a navigation controller called the "L1 controller" in the firmware "ArduPilot" which work together with the Pixhawk®. This controller produces much more accurate flight paths both for waypoints and loiter than the previous and PID controller. Anyway, there are hundreds of parameters used in the flight controller. It is nearly impossible to use traditional, one-factor-at-a-time (OFAT) and trial-and error experiments. Thus, a structure approach for conducting experiment such as Design of Experiment (DOE) is useful to model the relationships among the parameters, investigate the interaction between parameters and optimize the vehicle behaviors.

3. The Experimental System

3.1. A Scaled Boat

The objective of the experiment is to visualize the maneuvering behaviors. Therefore, direct observation of relevant conditions should be easy. It is convenient, faster, more flexibility and easier experimentation with less cost to use a small-scale boat. A 1/4 scaled boat has been decided and built with necessary hardware to serve as a plant for the control system with dimension about 0.79 m in length and 0.46 m in width as shown in Fig. 2.

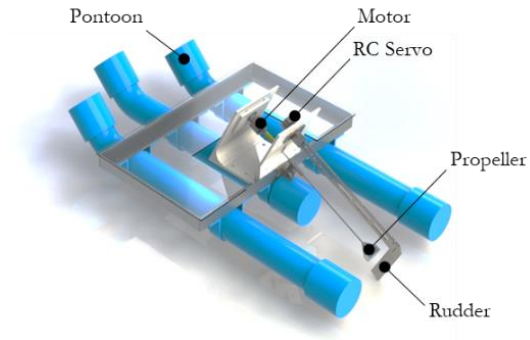

(a) The CAD model

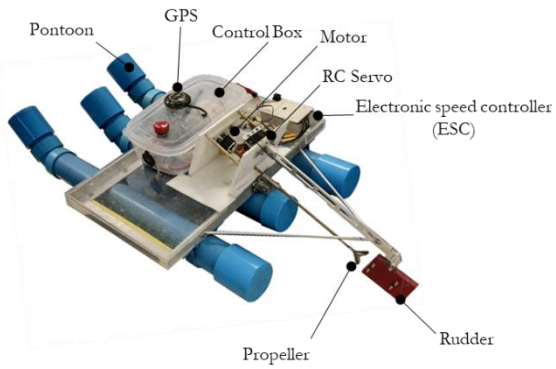

(b) The actual scaled boat

Fig. 2. A 1/4 scaled boat in the experiment.

The propulsion system is based on a brushless DC motor (BLDC) driven by an electronic speed controller (ESC). Heading control is done by moving the rudder with a RC servo. The control signal of the servo and ESC are well established PWM standards. So, they can be used for large servo and more powerful speed controller in the real scale boat with the same PWM signals. Therefore, our electronic system could equally be used in the real scale boat. Pixhawk® with internal accelerometer,

is used as the flight controller. The commonly used Ublox M8N GPS module with compass is connected to the flight controller. Together, the compass, accelerometer and GPS provide position, speed and heading to the control algorithms.

A 915 MHz telemetry radio allows the boat to communicate with the ground station. This allows interaction with the boat in real time and receive streaming data from the onboard sensors to the ground station. The range of radio link can reach up to 300 m without additional antenna or extend to several kilometers with the use of a patch antenna on the ground. However, all of the experiments were less than 50 m from the ground station.

A block diagram of the onboard electronic system is shown in Fig. 3.

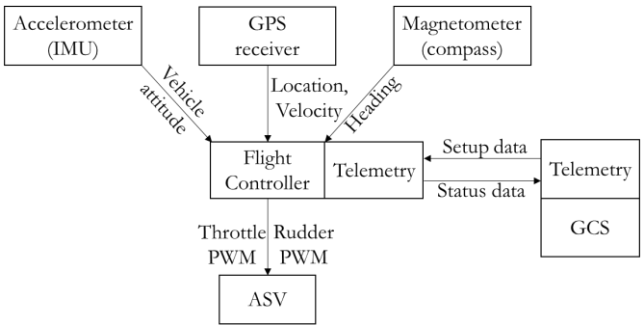

Fig. 3. Block diagram of the onboard electronic system.

3.2. Ground Control Station (GCS)

The software for the ground control station is "Mission Planner". The GCS communicates with the boat via wireless telemetry. Normally, the GCS is used for setting waypoints and parameters to the boat, before starting the operation. After that, it remains in passive mode for real-time data acquisitioning. Anyway, it is possible to modify the plan and parameters during the operation or use manual control to override the boat in case of unexpected problems. Google Maps is used as to perform plotting GPS traces and ASV motion.

3.3. Guidance, Navigation and Control

Since the boat has 2 degrees of freedom (throttle and rudder) as same as the rover (throttle and steering). So, it is possible to use the control algorithm in the same way with the rover. In this experiment, the control algorithm is based on the "ArduRover", an open-source autopilot for guiding ground vehicles.

There are 3 high level controllers: 1) The throttle controller, converts a desired speed into a throttle command. 2) The steering controller, converts a desired lateral acceleration, an angle error or a desired turn rate into a rudder output command. Steering control laws of the rudder are based on PID heading control with overshoot. And the L1 controller, converts an origin and destination (expressed in the latitude and longitude) into a lateral acceleration to make the vehicle travel along the path from the origin to the destination. This lateral acceleration is then passed into the steering controller.

4. Experimental Design

In this study, the researcher selected three parameters from the "ArduRover" control algorithm which may affect the maneuvering behaviors of the scaled boat. These parameters are *Pivot_Turn_Rate* (*T_Rate*), *Pivot_Turn_Angle* (*T_Angle*) and *NavL1_Damping* (*Damping*). Other parameters are set as default.

T_Angle holds the minimum angle error that will trigger the pivot turn. For example, when set to the default of "10", a pivot turn will be triggered whenever the boat's heading is at least 10 degrees off from the next waypoint with the desired turn rate *T_Rate*. The *Damping* is specified to compensate for delays in the velocity measurement. The response variable is the maneuvering behaviors observed by measuring the *peak-to-peak deviation* as shown in Fig. 4.

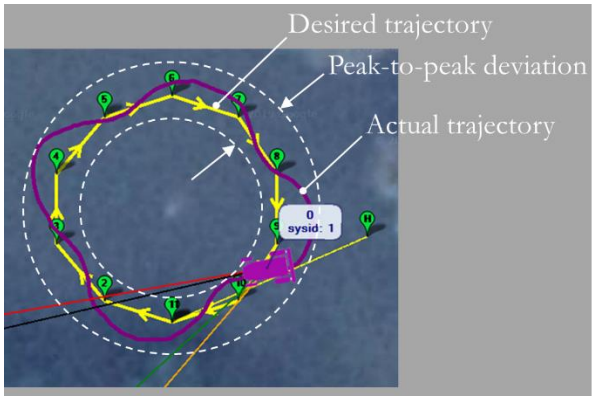

Fig. 4. Measurement of the peak-to-peak deviation.

A 2^3 full factorial design with 3 replications is carried out to study the influence of *T_Rate*, *T_Angle* and *Damping* on the response variable, *peak-to-peak deviation*, with general linear model under the assumptions that 1) the design is completely randomized, 2) the usual normality assumptions are satisfied, and 3) the response is approximately linear over the range of the factor levels chosen. Analysis of variance (ANOVA) is used to investigate and model the relationship between a response variable and one or more independent parameters.

Let the *T_Rate* be factor *A* with two levels of interest be 30 and 40 deg/s. The *T_Angle* is factor *B*, with two levels of interest be 5 and 10 deg. The *Damping* is factor *C*, with the high level 0.95 and low level 0.85. The experiment is replicated three times, so there are 24 runs, made in random order to prevent the effects of unknown nuisance variables. Eight treatment combinations can be displayed geometrically as a cube, as shown in Fig. 5.

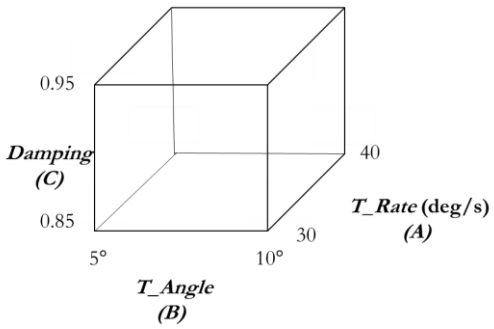

Fig. 5. A three-factor factorial experiment involving *T_Rate (A)*, *T_Angle (B)* and *Damping (C)*.

5. Results

With the desired trajectory as a circle with 20 m in diameter with 10 waypoints, the observation of *peak-to-peak deviation* are shown in Table 1.

Table 1. Peak-to-peak deviation from experiments.

Run no.	*A*	*B*	*C*	Peak-to-peak dev. (m)		
				1	2	3
1	30	5	0.85	6.30	4.85	6.16
2	40	5	0.85	4.80	2.45	5.08
3	30	10	0.85	4.07	1.97	3.68
4	40	10	0.85	6.41	4.33	4.78
5	30	5	0.95	4.41	4.04	3.68
6	40	5	0.95	2.87	3.90	3.33
7	30	10	0.95	3.21	4.23	3.63
8	40	10	0.95	4.09	3.94	3.86

5.1. Analysis of Variance (ANOVA)

ANOVA is used to investigate and model the relationship between a response variable and one or more independent parameters. In this study, the significant level $\alpha = 0.05$ has been selected. The result of ANOVA is summarized in Table 2.

Table 2. Result of ANOVA.

Source	DF	Adj. SS.	Adj. MS.	F-value	P-value
Model	7	16.1090	2.30129	3.15	0.027
A	1	0.0063	0.00634	0.01	0.927
B	1	0.5612	0.56120	0.77	0.394
C	1	3.9123	3.91234	5.35	0.034
AB	1	7.7407	7.74070	10.59	0.005
AC	1	0.1717	0.17170	0.23	0.634
BC	1	1.0965	1.09654	1.50	0.238
ABC	1	2.6202	2.62020	3.58	0.077
Error	16	11.6945	0.73090		
Total	23	27.8035			

The *AB* interaction has a P-value of 0.005, indicating a strong interaction between these factors. From Fig. 6, the normal probability plot shown that the error distribution is approximately normal. There is also no violation of the independence or constant variance assumptions from residuals versus observation order. Residuals versus fitted value reveal no unusual pattern, implied that the data are scattered and unrelated to any variable including the response.

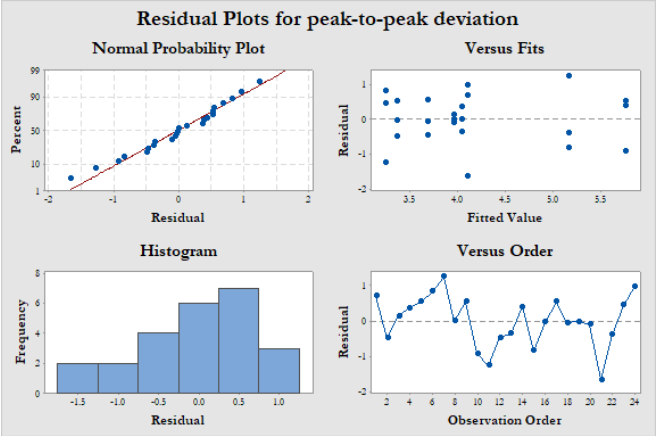

Fig. 6. Residual plots for peak-to-peak deviation.

5.2. Main and Interaction Effects

From Fig. 7, the interaction between *T_Rate* and *T_Angle* (*AB*) and the main effect of *Damping* (*C*) are statistically significant at 95% confident. On the normal probability plot, the *AB* interaction has positive standardized effect. When the *AB* interaction increase, the peak-to-peak deviation increases. While Fig. 8 shows that all three variables have negative main effects; the peak-to-peak deviation decrease while increasing the variables.

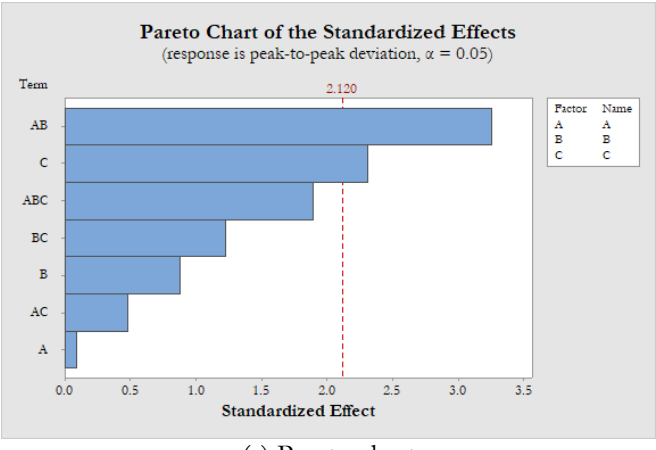

(a) Pareto chart

DOI:10.4186/ej.2020.24.5.217

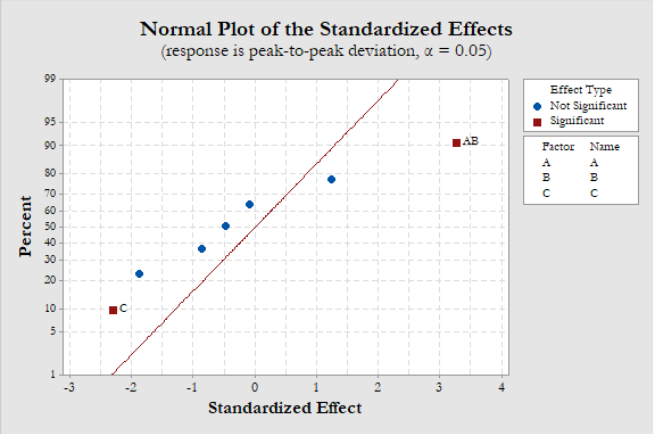

(b) Normal probability plot

Fig. 7. The standardized effects.

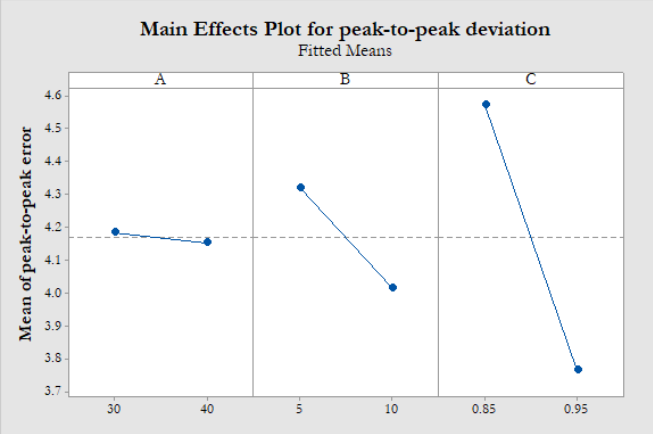

Fig. 8. Main effects plot for peak-to-peak deviation.

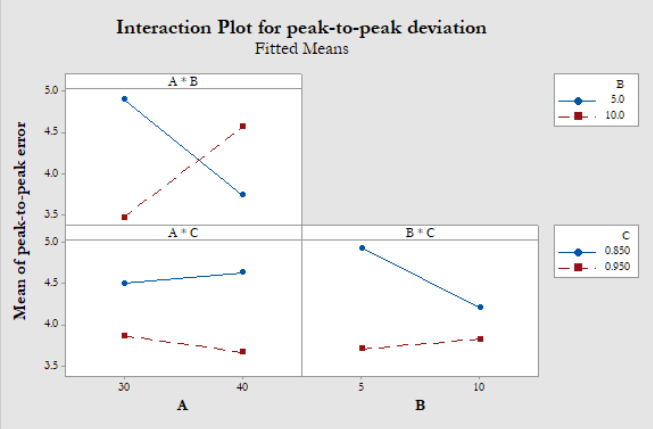

Fig. 9. Interaction plot.

The crossed lines on the interaction plot (Fig. 9) suggest that there is an interaction effect between *A* and *B*, which confirm with the P-value and pareto chart of the standardized effects. The graph shows that the peak-to-peak deviation are lower for low-level *T_Rate* (*A*) and high-level *T_Angle* (*B*). The nonparallel lines between *AC* and *BC* indicate that there is some interaction between *T_Rate*Damping* and *T_Angle*Damping*.

5.3. Regression Model

The regression model representation of the three-factor factorial experiment could be written as:

$$y = \beta_0 + \beta_1 A + \beta_2 B + \beta_3 C + \beta_{12} AB + \beta_{13} AC + \beta_{23} BC + \beta_{123} ABC + e \quad (1)$$

where y is the response (*peak-to-peak deviation*), the β are parameters whose values are to be determined, A is a variable that represent *T_Rate*, B is a variable that represent *T_Angle*, C is a variable that represent *Damping*. AB, AC, BC and ABC represents the interaction between A and B, A and C, B and C, A and B and C respectively. e is a random error.

Therefore, the fitted regression model could be expressed as:

$$\hat{y} = 149.7 - 3.61A - 19.84B - 147.8C + 0.521AB + 3.63AC + 20.21BC - 0.529ABC \quad (2)$$

However, the interaction AC, BC and ABC are small as shown in Fig. 7(a) and indicated by nonparallel lines in Fig. 9. Therefore, dropping these three, the model becomes:

$$\hat{y} = 23.94 - 0.344A - 1.651B - 8.08C + 0.0454AB \quad (3)$$

With the fitted regression in Eq. (3), the new residual plot can be shown in Fig. 10.

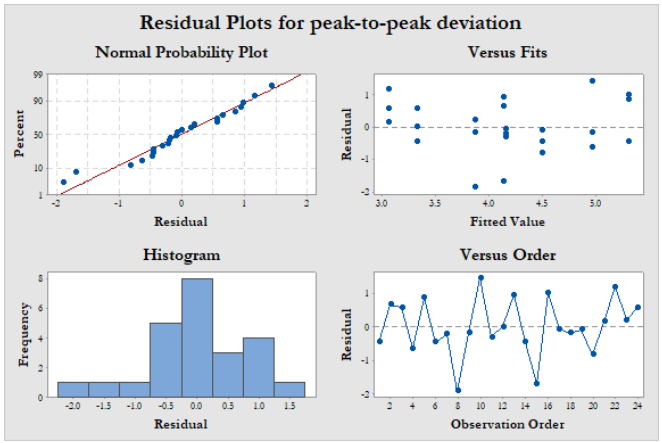

Fig. 10. Residual plots for peak-to-peak deviation of the fitted regression.

Since *Damping* (*C*) shows a small interaction with *T_Rate* (*A*) and *T_Angle* (*B*) and we want the error as low as possible, we decided to use the high level of *Damping* (0.95). By substituting $C = 0.95$ into Eq. (3), the result is

$$\hat{y} = 16.264 - 0.344A - 1.651B + 0.0454AB \quad (4)$$

The ANOVA of the new fitted regression in Eq. (4) is summarized in Table 3.

Table 3. Result of ANOVA of the fitted regression.

Source	DF	Adj. SS.	Adj. MS.	F-value	P-value
Model	4	12.2206	3.05515	3.73	0.021
A	1	0.0063	0.00634	0.01	0.931
B	1	0.5612	0.56120	0.68	0.418
C	1	3.9123	3.91234	4.77	0.042
AB	1	7.7404	7.74070	9.44	0.006
Error	19	15.5829	0.82015		
Lack-of-Fit	3	3.8884	1.29615	1.77	0.193
Pure Error	16	11.6945	0.73090		
Total	23	27.8035			

5.4. Response Surface

Equation (4) can be used to generate the response surface plot as shown in Fig. 11.

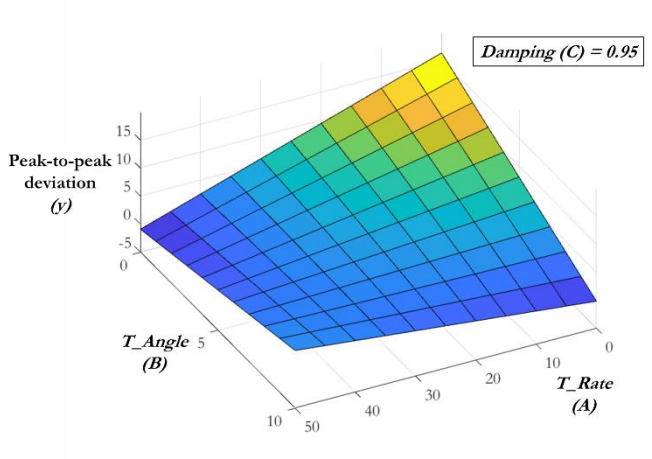

(a) Response surface

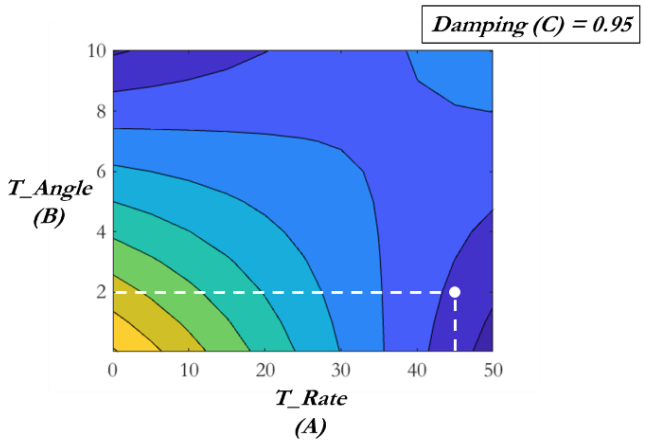

(b) Contour plot

Fig. 11. Response surface of *peak-to-peak deviation* as a function of *T_Rate* and *T_Angle* with *Damping* 0.95.

From Eq. (4) and the response surface in Fig. 11, the *T_Rate* (*A*) and *T_Angle* (*B*) have been set to 45 deg/s and 2 degree respectively for better maneuvering (high turn rate) with *Damping* equal to 0.95. The predicted peak-to-peak deviation becomes 1.57 m.

After that, the boat was set with these optimized parameters and perform the experiment with three replications. The result was shown in Table 4 and Fig. 12.

Table 4. Experimental results compared with the fitted regression with new parameters.

Parameter setting					
T_Rate	45 deg/s				
T_Angle	2 deg				
Damping	0.95				
Peak-to-peak deviation (m)					
Test no. 1	Test no. 2	Test no. 3	Avg.	From regression	Error
1.68	2.62	2.01	2.10	1.57	25%

The result shown that with a new set of parameters, the peak-to-peak deviation can be reduced to approximately 2 m. The error is about 25% from the regression model.

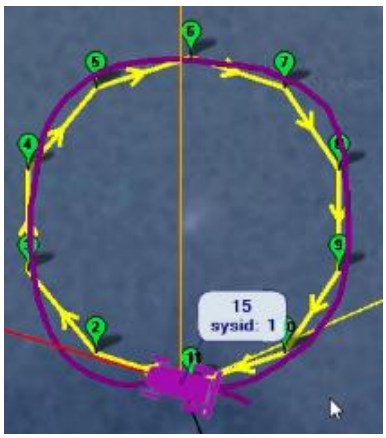

Fig. 12. Trajectory of the boat after tuning.

Fig. 13. The autonomous boat on the field test.

Through field tests conducted at Mahidol University during March and April 2019 (Fig. 13), the boat can run in manual mode receiving the user input remotely. The controls feel responsive with acceptable maneuvering

behaviours. From the user experience gained during the test, the response of the system can be improved further by improving the throttle power and the rudder effectiveness.

When the autonomous system is activated, the control algorithm on the embedded controller together with various sensors performed in a satisfactory manner, enabling the autonomous operation of the boat.

6. Conclusions

A small-scale pontoon boat has been built, equipped with the open-hardware flight controller, GPS receiver, Inertial Measurement Units (IMU) and the magnetometer to convert to an autonomous boat. It is capable of maneuvering a predefined path with no user intervention.

The effect of three parameters of the control algorithm has been investigated. The experiments were based on a two-level factorial design to be able to develop a regression model for a peak-to-peak deviation in maneuvering as a response.

It is found that the parameter *Damping* has low interaction with the *T_Angle* and *Turn_Rate* while there is a stronger interaction between *T_Angle* and *Turn_Rate*. The peak-to-peak deviation of the trajectory tend to decrease when the parameter *Damping* was set to high value (0.95).

With *Damping* set as a constant at 0.95, the fitted regression and the response surface suggest that 1.57 m peak-to-peak deviation can be achieved with *T_Rate* of 45 deg/s and *T_Angle* of 2 degree. Finally, the optimum parameters have been used to perform additional experiments to validate the model. Comparison of the results confirms that the tuning with DOE have improved the accuracy and performance of the autonomous small-scale boat.

References

[1] Food and Agriculture Organization of the United Nations. (2019). *FAO's Role in Aquaculture* [Online]. Available: http://www.fao.org/aquaculture/en/ [Accessed: 2 December 2019]

[2] G. Kumar and C. R. Engle, "Technological advances that led to growth of shrimp, salmon, and tilapia farming," in *Reviews in Fisheries Science & Aquaculture*, vol. 24, no. 2, pp. 136-152, 2016.

[3] P. Rogers, "Economy of scales," *Stanford Magazine*. 2006.

[4] J. E. Rakocy, "Cultured aquatic species information programme. Oreochromis niloticus," FAO Fisheries and Aquaculture Department, 2005.

[5] Y. J. Mallya and H. Thorarensen, "The effects of dissolved oxygen on fish growth in aquaculture," in *UNU-Fisheries Training Program*. Reykjavik, Iceland: The United National University, 2007, pp. 1-30.

[6] R. M. Abou Zied, "Effect of aeration systems and stocking density on growth performance, pond yield and economic impacts of Nile Tilapia (Oreochromis niloticus) reared in earthen ponds," *Abbassa Int. J. Aqua*, vol. 6, no. 1, pp. 213-228, 2013.

[7] J. Kepenyes and L. Varadi, "Aeration devices for fish ponds," in *Aeration and Oxygenation in Aquaculture*. Szavas, Hungary: Fish Culture Research Institute, 1984.

[8] C. E. Boyd, "Source water, soil and water quality impacts on sustainability in aquaculture," in *Pacific Congress on Marine Science and Technology*, Honolulu, 1995.

[9] T. Sultana, M. Haque, M. Salam and M. M. Alam. "Effect of aeration on growth and production of fish in intensive aquaculture system in earthen ponds," *Journal of the Bangladesh Agricultural University*, vol. 15, pp. 113-122, 2017.

[10] V. P. Agrawal, "Recent Trends in Aquaculture," Society of Biosciences, 1999.

[11] A. Bergheim, M. Gausen, A. Næss, P. M. Hølland, P. Krogedal, and V. Crampton, "A newly developed oxygen injection system for cage farms," *Aquacultural Engineering*, vol. 34, no. 1, pp. 40-46, 2006.

[12] H. A. Loyacano, "Effects of aeration in earthen ponds on water quality and production of white catfish," *Aquaculture*, vol. 3, no. 3, pp. 261-271, 1974.

[13] T. B. Lawson, "Water Quality and Environmental Requirements," in *Fundamentals of Aquacultural Engineering*. Springer Science & Business Media, B.V, 1995.

[14] C. E. Boyd, "Advances in pond aeration technology and practices," *INFOFISH International*, vol. 2, pp. 24-28, 1997.

[15] M. Harris. (2014), *Aeration systems: How they improve your pond or lake* [Online]. Available: https://www.solitudelakemanagement.com/blog/aeration-systems-how-they-improve-your-pond-or-lake- [Accessed: 2 December 2019]

[16] Food and Agriculture Organization of the United Nations. (n.d.). *Controlling water losses in ponds* [Online]. Available: http://www.fao.org/tempref/FI/CDrom/FAO_Training/FAO_Training/General/x6709e/x6709e03.htm [Accessed 2 December 2019]

[17] C. E. Boyd, "Sediment," in *Bottom Soils, Sediment, and Pond Aquaculture*. New York: Chapman & Hall, 1995, ch. 7.

[18] Shrimp Center. (n.d.). *Dragging chain: Controlling plankton blooms in aquaculture* [Online]. Available: https://www.shrimpcenter.com/t-shrimp038.html [Accessed 3 December 2019]

[19] Agricultural Research Development Agency. (n.d.). *Underwater ploughing pontoon boat* [Online]. Available: http://www.arda.or.th/kasetinfo/south/shrimp/controller/machinery6.php [Accessed 2 December 2019]

[20] A. Tunsutapanich, S. Thongrod, T. Sanggontanagit, and C. Omanee, "Improvement techniques for seed

producing and nursing giant prawn (Macrobrachium rosenbergii de Man) larvae in Earthen pond in closed system," *Warasan Kan Pramong*, vol. 50, no. 1, pp. 67-78, 1997.
[21] A. Tunsutapanich, T. Sanggontanagit, T. Permngarm, and C. Omanee, "Study on elimination of pollutants in closed culture system of giant tiger shrimp (Penaeus monodon)," *Warasan Kan Pramong*, vol. 51, no. 3, pp. 203-209, 1998.
[22] Diversified Pond Supplies LLC. (n.d.). *Earthen ponds frequently asked questions* [Online]. Available: https://www.diversifiedpondsupplies.com/earthen-ponds-frequently-asked-questions [Accessed 2 December 2019]
[23] D. J. Yost, J. E. Kain, "Command to line-of-sight guidance: A stochastic optimal control problem," *Journal of Spacecraft*, vol. 17, no. 7, pp. 438-444, 1977.
[24] J. H. Blakelock, "Guidance systems," in *Automatic Control of Aircraft and Missiles*, 2nd ed. Wiley-Interscience, 1991, ch. 8, sec. 8.2, pp. 262-272.
[25] P. Zarchan, "Other forms of tactical guidance," in *Tactical and Strategic Missile Guidance*, 6th ed. AIAA, 1997, ch. 10, pp. 165-192.
[26] P. Sanghyuk, D. John, and P. H. Jonathan, "A new nonlinear guidance logic for trajectory tracking," in *AIAA Guidance, Navigation, and Control Conference and Exhibit*, Rhode Island, 2004, pp. 1-16.
[27] R. Stelzer and T. Pröll, "Autonomous sailboat navigation for short course racing," *Robotics & Autonomous Systems*, vol. 56, no. 7, pp. 604-614, 2008.
[28] N. A. Cruz and J. C. Alves, "Auto-heading controller for an autonomous sailboat," in *OCEANS 2010 IEEE*, Sydney, 2010, pp. 1-6.
[29] B. Clement, "Control algorithms for a sailboat robot with a sea experiment," *IFAC Proceedings*, vol. 46, no. 33, pp. 19-24, 2013.
[30] P. Velaskar, A. Vargas-Clara, O. Jameel, and S. Redkar, "Guided navigation control of an unmanned ground vehicle using global positioning systems and inertial navigation systems," *International Journal of Electrical and Computer Engineering,* vol. 4, no. 3, pp. 329-342, Jun. 2014.
[31] S. Ullah and W. Abdullah, "Autonomous Surveying Boat," *ArXiV*, 2014.
[32] J. M. Giron-Sierra, A. T. Gheorghita, G. Angulo, and J. F. Jimenez, "Preparing the automatic spill recovery by two unmanned boats towing a boom: Development with scale experiments," *Ocean Engineering*, vol. 95, pp. 23-33, 2015.
[33] H. S. Stenersen, "Construction and control of an autonomous sail boat," *IFAC-PapersOnLine*, vol. 49, no. 23, pp. 524-531, 2016.
[34] G. Zhang and L. T. Hsu, "Intelligent GNSS/INS integrated navigation system for a commercial UAV flight control system," *Aerospace Science & Technology*, vol. 80, pp. 368-80, Sep. 2018.

Mongkol Thianwiboon was born in Lampang Thailand in 1976. He received the B.S. and M.S. and the Ph.D. degrees in mechanical engineering from Chulalongkorn University in 1997, 2000 and 2005 respectively.

From 2000 to 2005, he was a system administrator at Engineering Computer Center, Chulalongkorn University while studying the Ph.D. degree. After that, he worked with Lenso Wheel Co., Ltd as a project engineer during 2005 to 2008. Later, he was the manager of the Process Improvement Department during 2008 to 2011. Since 2011, he has been an faculty member of the Industrial Engineering Department, Mahidol University. His research interests include robotic and autonomous system and computational fluid dynamics.

Dr. Thianwiboon is a member of the Council of engineers and Society of Automotive Engineers -Thailand (TSAE).